Available online at www.sciencedirect.com
ScienceDirect
Journal of Virological Methods 138 (2006) 160–169
Journal of Virological Methods
www.elsevier.com/locate/jviromet

Control of antigen mass transfer via capture substrate rotation: An absolute method for the determination of viral pathogen concentration and reduction of heterogeneous immunoassay incubation times

Jeremy D. Driskell [a], Karen M. Kwarta [a], Robert J. Lipert [a], Ann Vorwald [b], John D. Neill [b], Julia F. Ridpath [b], Marc D. Porter [a,*]

[a] *Iowa State University, Institute for Combinatorial Discovery, Departments of Chemistry and Chemical and Biological Engineering, The Ames Laboratory-USDOE, Ames, IA 50011-3020, United States*
[b] *Virus and Prion Diseases of Livestock Unit, National Animal Disease Center, United States Department of Agriculture, Ames, IA 50010, United States*

Received 26 April 2006; received in revised form 7 August 2006; accepted 29 August 2006
Available online 10 October 2006

Abstract

Immunosorbent assays are commonly employed as diagnostic tests in human healthcare, veterinary medicine and bioterrorism prevention. These assays, however, often require long incubation times, limiting sample throughput. As an approach to overcome this weakness, this paper examines the use of rotating capture substrates to increase the flux of antigen to the surface, thereby reducing the incubation time. To assess the capability of this approach, porcine parvovirus (PPV) was selectively extracted from solution by systematically varying the rotation rate of a gold substrate modified with a layer of anti-PPV monoclonal antibodies. The captured PPV were then directly imaged and quantified by atomic force microscopy. The benefits of substrate rotation are demonstrated by comparing an assay performed under stagnant conditions to one carried out with substrate rotation at 800 rpm, both for 10 min incubations at 25 °C. The use of rotation lowered the limit of detection to 3.4×10^4 $TCID_{50}$/mL (~80 fM) from 3.2×10^5 $TCID_{50}$/mL (~800 fM) under stagnant conditions. Results are also presented that show this strategy can be used: (1) to determine antigen concentrations without standards and (2) to establish the numerical relationship between quantal concentration units (e.g., 50% tissue culture infective dose ($TCID_{50}$)) and quantitative concentration units (e.g., viruses/mL) The potential to broadly apply this technique to heterogeneous immunoassays is also briefly discussed.

Keywords: Immunoassay; Induced flux; PPV; Atomic force microscopy

1. Introduction

Immunoassay development continues to be one of the most active areas at the interface between the analytical and biological sciences (Diamandis and Christopoulos, 1996; White et al., 2000). This situation results in large part from the ever-increasing demand for diagnostic tests in human healthcare and veterinary medicine that enhance throughput, simplify sample workup, reduce analysis time and lower the level of detection. Advances to these ends will not only improve chances for early diagnosis and thereby increase the likelihood of successful treatment and recovery, but also reduce the potential spread of disease and decrease the length of possible hospitalization (Sokoll and Chan, 1999). These advances are also central to addressing challenges in bioterrorism prevention (Chomel, 2003).

Recent breakthroughs in electrochemical, optical, magnetic, scanning probe microscopic and several other detection modalities are poised to meet these needs (Cao et al., 2002; Cousino et al., 1997; Donaldson et al., 2004; Driskell et al., 2005; Ferguson et al., 2000; Grubisha et al., 2003; Kjeldsberg, 1986; Llic et al.,

* Corresponding author. Present address: Center for Combinatorial Chemistry, The Biodesign Institute and Department of Chemistry and Biochemistry, Arizona State University, 1001 South McAllister, Mail Code 6401, Tempe, AZ 85287. Tel.: +1 480 727 8598; fax: +1 480 727 9499.
E-mail address: marc.porter@asu.edu (M.D. Porter).

0166-0934/$ – see front matter © 2006 Elsevier B.V. All rights reserved.
doi:10.1016/j.jviromet.2006.08.011

2004; Nettikadan et al., 2003; Richardson et al., 2001; Wang and Branton, 2001; Zheng et al., 1999). These developments have pushed the limit of detection to femtomolar levels and lower. However, when the mass transfer of analyte is governed solely by diffusion, incubation times of several hours may be required when analyzing biological samples. This situation arises because diffusion coefficients for proteins and other large biolytes can be a few orders of magnitude lower than those for small molecules (Sheehan and Whitman, 2005). The challenge then is to develop strategies that rapidly transport the antigen to the capture substrate in order to take advantage of the emerging breakthroughs in ultra-low levels of detection. Moreover, the potential to capitalize on enhancements in the flux of antigen is supported by research that has repeatedly shown that the rate of heterogeneous antibody–antigen binding is limited by antigen mass transport rather than by binding kinetics (i.e., recognition rate) (Frackelton and Weltman, 1980; Myszka et al., 1997; Nygren et al., 1987; Stenberg and Nygren, 1985; Stenberg et al., 1986).

Several laboratories have examined methods aimed at decreasing incubation times by increasing the flux of analyte to the capture substrate. Approaches include electric field-driven transport (Ewalt et al., 2001; Heller et al., 2000), confinement of the fluid flow profile to a thin layer above a capture antibody substrate (Glaser, 1993; Hofmann et al., 2002) and elevations in temperature (Johnstone et al., 1990) to decrease solution viscosity. The work presented in this paper utilizes the rotation of capture antibody substrates as a means to increase the flux of antigen to the surface. Rotation is a well characterized method of quantitatively controlling flux to a surface, and has historical precedence in electrochemistry where rotating disk electrodes (RDE) are often used as a facile means to manipulate mass transport in studies of electrode reaction mechanisms. RDEs have also been employed in immunoassays during the amperometric detection step of redox probes that were generated by an enzymatic label in a sandwich-type assay (Messina et al., 2005; Salinas et al., 2005; Wijayawardhana et al., 1999). To our knowledge, only one example has taken advantage of rotation as a means to increase the flux of antigen to the capture substrate (Huet et al., 1990). The goal of that study, however, was solely to control mass transport in order to develop an assay in which the quantitative detection of antigen binding was independent of sample volume. The initial aim of the work herein was to reduce incubation times for the ultra-low level detection of viruses; a goal that, as we will show, was achieved.

This paper also reports on another interesting development-rotation-induced flow facilitates the accurate determination of virus concentration without standards. Typically, virus concentrations are estimated with quantal rather than quantitative techniques (Murphy et al., 1999). These techniques, which include infectious and hemagglutination titrations and plaque assays, approximate virus concentrations in units of 50% tissue culture infective dosage ($TCID_{50}$), hemagglutination units (HA) or plaque-forming units (PFU), respectively. While quantal techniques have proven highly effective, concentrations given as the number of virus particles per unit volume represent a more effective means for assessment of assay performance and, ultimately, diagnostic utility.

At present, transmission electron microscopy (TEM) is the standard for the measurement of virus concentration in terms of virus particles per unit volume (Wagner and Hewlett, 1999). This method requires drying a known volume of virus on a TEM grid, enumerating the viruses in a well defined area on the grid, and extrapolating this value to represent the number of viruses on the droplet-coated surface. However, the reliable implementation of this approach requires highly purified virus solutions and the accurate transfer and uniform drying of small sample volumes to the TEM grid. The combined weight of these factors severely limits the reliability of this method (Wagner and Hewlett, 1999).

The results in this paper show that rotating capture antibody substrates markedly lowers the time required for sample incubation, lowers the limit of detection, and can be used to determine virus concentration as viruses per unit volume. This capability can also be employed to determine the relationship between the quantal units per unit volume (i.e., $TCID_{50}$, HA and PFU) and viruses per unit volume. Evaluation of our approach was performed with the capture of porcine parvovirus (PPV) (~25 nm diameter) on a rotating capture substrate. The capture substrate, which has been previously constructed in our laboratory (Driskell et al., 2005), has an anti-PPV monoclonal antibody (mAb) covalently coupled to a gold surface through a thiolate adlayer formed from dithiobis(succinimidyl propionate). The capture substrate is then attached to a rotating rod and submerged in sample solution. After extraction, the captured viruses are directly enumerated utilizing an atomic force microscope (AFM). The capability of AFM as a label-free analytical tool for imaging nanometer-sized objects, such as viruses, has recently been demonstrated (Driskell et al., 2005; Kuznetsov et al., 2001; Nettikadan et al., 2003); however, many other quantitation methods (e.g., electrochemical, optical, magnetic, etc.) could also be used. The experiments described herein were designed to examine the effect of substrate rotation rate and sample incubation time on the amount of virus bound to the capture platform as well as to quantitatively compare immunoassay performance with rotation to that under stagnant conditions. The findings of these experiments, which include tests for binding specificity, are also discussed in light of theoretical expectations derived from established RDE theory.

2. Theory

The flux of material delivered to a rotating, planar substrate can be quantitatively formulated for systems which meet the following criteria: (1) the bulk concentration of analyte in the sample solution is constant over the course of the experiment; (2) the rate of the reaction at the substrate surface is mass transport limited (rather than antibody–antigen recognition rate limited). With these boundary conditions, theoretical treatments have been developed to accurately describe the mass transfer of analyte to an electrode surface for a wide range of electrochemical processes (Opekar and Beran, 1976). The same theory can be applied to a heterogeneous immunoassay provided that: (1) binding sites on the capture substrate are not saturated with antigen; (2) bulk antigen concentration in the sample solution does not vary during the time of incubation; (3) antibody–antigen

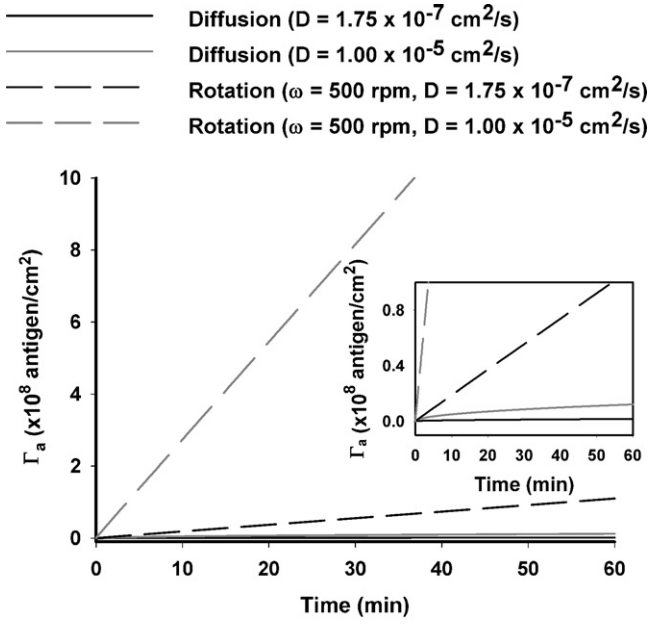

Fig. 1. Calculated antigen surface concentration accumulated as a function of time, antigen diffusion coefficient and substrate rotation.

binding step is much faster than the delivery of antigen to the substrate. As we will show, the resulting theory allows the quantity of extracted antigen to be predicted, highlighting both the importance of the antigen diffusion coefficient and the need for increased mass transport for large molecules.

Using these boundary conditions, the diffusional flux of antigen to the sensing surface (J_{diff}) and the accumulated surface concentration (Γ_a) of the antigen over time can both be calculated by modified forms of the Cottrell equation (Bard and Faulkner, 2001; Rieger, 1994), and are given by Eqs. (1) and (2), respectively

$$J_{Diff} = \frac{1}{\pi} D^{1/2} C_b t^{-1/2} \quad (1)$$

$$\Gamma_a = \frac{2}{\pi} D^{1/2} C_b t^{1/2} \quad (2)$$

where D is the diffusion coefficient of the antigen, C_b the bulk antigen concentration and t is the time. These equations indicate that the delivery and accumulation of antigen at the surface of a capture substrate are directly proportional to $D^{1/2}$. This dependence indicates that a 100-fold difference in the diffusion coefficient of the antigen translates to a 10-fold difference in antigen accumulation. Moreover, Eq. (2) shows that accumulation increases with $t^{1/2}$.

Fig. 1 plots the accumulation of antigen ($C_b = 1.00 \times 10^8$ antigen/mL) at a surface as a function of time, calculated using Eq. (2), for two different diffusion coefficients, one typical of a small molecule ($D = 1.00 \times 10^{-5}$ cm^2/s) and the other exemplifying a large analyte ($D = 1.75 \times 10^{-7}$ cm^2/s). It is evident that Γ_a increases much faster for the small molecule compared to the large molecule, illustrating the significance of incubation time prior to readout and the need for increased mass transport in the case of a large analyte.

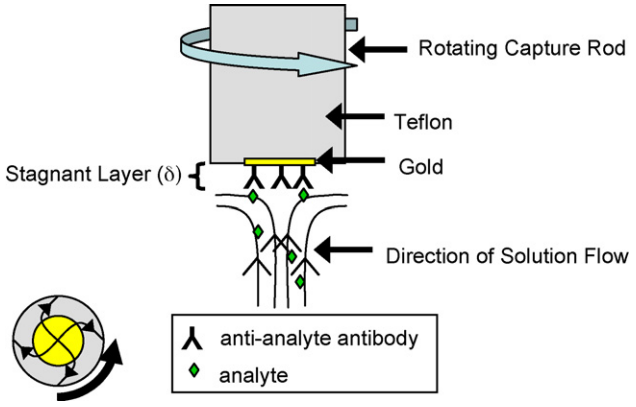

Fig. 2. Schematic of solution flow in the presence of a rotating capture rod.

As noted earlier, a rotating disk configuration is an effective and facile means in which to manipulate the rate of antigen binding because the hydrodynamic conditions that quantitatively control the flux of material to a planar substrate can be readily formulated. Fig. 2 depicts the key concepts of the system hydrodynamics, which involve convective mass transfer to establish steady-state conditions. As such, a rotating rod stirs the bulk solution at a carefully controlled and constant rate while delivering it to the surface of the disk at a quantifiable rate. Rotation also sets up a stagnant layer of solution at the disk surface, commonly referred to as the diffusion layer (δ); the analyte must diffusively pass through this layer to reach the disk. The convective flux induced by rotation can be formulated by starting with Eq. (3) (Bard and Faulkner, 2001; Rieger, 1994).

$$J_{conv} = \frac{D}{\delta} C_b \quad (3)$$

Importantly, the thickness of δ is controlled by rotation rate; larger rotation rates decrease the thickness, increasing the flux of the analyte.

The thickness of the diffusion layer as a function of rotation velocity, as developed in a model by Levich (1962), is given by

$$\delta = 1.61 V^{1/6} D^{1/3} \omega^{-1/2} \quad (4)$$

where V represents the kinematic viscosity of the sample solution and ω is the angular rotation rate of the substrate (radians/s). Eqs. (3) and (4) can be combined to provide an expanded description of antigen flux to the substrate for the steady-state case imposed by substrate rotation. This step yields

$$J_{conv} = \frac{D^{2/3} C_b}{1.61 V^{1/6}} \omega^{1/2} \quad (5)$$

Ultimately, Γ_a can be formulated by integrating the total flux with respect to the incubation time to give

$$\Gamma_a = \frac{2}{\pi} D^{1/2} C_b t^{1/2} + \frac{D^{2/3} C_b}{1.61 V^{1/6}} t\omega^{1/2} \quad (6)$$

The first term in Eq. (6) accounts for the antigen accumulation in the absence of a steady-state delivery of solution (i.e., no rotation), but is quickly dominated by the second term once steady-state is obtained (i.e., rotation).

Eq. (6) shows that for a given sample, Γ_a is dependent upon incubation time and rotation rate but not on sample volume. Using a rotation rate of 500 rpm, the comparisons in Fig. 1 demonstrate that the accumulation of both large and small antigens on the surface is markedly enhanced by substrate rotation. In both cases, the improvements are directly proportional to $\omega^{1/2}$. These predictions therefore argue that the time required to carryout immunoassays typically performed under stagnant conditions can be immensely reduced without sacrificing, and potentially lowering, the limit of detection. Furthermore, for systems accurately described by Eq. (6), if D is known and t and ω are controlled, it should be possible to quantitate the antigen concentration, C_b, without the use of standards by measuring Γ_a.

3. Experimental

3.1. Reagents

Octadecanethiol (ODT), dithiobis(succinimidyl propionate) (DSP) and phosphate-buffered saline (PBS) packs (10 mM) were purchased from Sigma. Borate buffer packs (50 mM) were acquired from Pierce. Contrad 70 (Micro, Cole-Parmer) was used for cleaning glass substrates and two-part epoxy (Epoxy Technology) was employed to construct template stripped gold. All buffers were passed through a 0.22 μm syringe filter (Costar) before use. Poly(dimethyl siloxane) (PDMS) was obtained from Dow Corning.

Anti-PPV monoclonal antibodies (1 mg/mL), supplied by National Animal Disease Center (NADC; Ames, IA, USA), were purified with a protein G column (Pro-Chem) and stored in 10 mM PBS. Anti-feline calicivirus (FCV) monoclonal antibodies (1 mg/mL), also protein G purified, were provided by NADC for use in control studies demonstrating the binding specificity of the capture substrate. Aliquots of purified PPV, suspended in 10 mM PBS, were also provided by NADC. Detailed procedures for the generation of the antibodies and the virus have been previously reported (Mengeling et al., 1988). The PPV concentration of the stock solution was determined from titrations to be 3.2×10^9 $TCID_{50}$/mL using the Reed–Muench method (Reed and Muench, 1938). All dilutions of the PPV stock solution were made with 10 mM PBS.

3.2. Capture substrate preparation/immunoassay protocol

Template stripped gold (TSG) (Stamou et al., 1997) served as the base for fabrication of the capture substrate, noting that its low roughness factor (0.6 nm) facilitated the enumeration of PPV (hydrated diameter of ~25 nm) by AFM (Driskell et al., 2005; Nettikadan et al., 2003). To prepare TSG, 250 nm of gold (99.9% purity) were resistively evaporated onto a 4 in. p-type silicon[1 1 1] wafer (University Wafer) at a rate of 0.1 nm/s using an Edwards 306A resistive evaporator. Next, 1 cm × 1 cm glass squares, cut from microscope slides (Fisher Scientific), were ultrasonically bathed in diluted Contrad 70, deionized water and ethanol, each for 30 min. Epoxy cement was applied to one side of the clean glass chips, which were then affixed to the gold-coated silicon wafer and cured at 150 °C for ~100 min. After curing, the glass chips were carefully detached from the wafer, a process that exposes a smooth gold surface.

TSG was exposed for ~30 s to an ODT-saturated PDMS stamp with a 4 mm hole cut in its center, then rinsed with ethanol, and dried under a stream of high purity nitrogen (Chen et al., 1998; Kumar and Whitesides, 1993; Libioulle et al., 1999). This procedure forms an ODT-derived monolayer, which provides a circular hydrophobic barrier to localize reagents on the center of the substrate in subsequent steps and minimize both reagent and sample consumption. Next, the ODT-inked substrate was submerged in a 0.1 mM ethanolic DSP solution for ~12 h, rinsed with ethanol and dried under a stream of high purity nitrogen. This process forms a DSP-based adlayer in the center of the substrate, which was not exposed to ODT in the stamping process.

Anti-PPV mAbs (20 μL), diluted to 100 μg/mL in 50 mM borate buffer (pH 8.5), were pipetted onto the center of the substrate and allowed to react for 8 h in a humidity chamber at room temperature. This step forms a capture antibody layer due to the amide linkage that arises from the reaction of the primary amines on the mAbs to the succinimidyl ester of the DSP-derived monolayer (Duhachek et al., 2000; Jones et al., 1998; Wagner et al., 1996). The substrate was immersed in 10 mM PBS (2.5 mL) three times to remove unreacted mAbs. After rinsing, the back of the capture substrate was quickly dried and attached to an RDE with double-sided tape while maintaining a thin layer of buffer on the topside of the substrate in order to ensure continual hydration of the mAbs. The RDE-mounted substrate was then loaded into a Pine analytical rotator (AFMSRX) and lowered into a 1.0 mL sample containing PPV. All sample volumes were held constant at 1.0 mL and all incubations were performed at room temperature. After incubation, the substrate was rinsed three times with 2.5 mL of PBS, exposed to a gentle flow of deionized water to remove residual salts, dried with a stream of high purity nitrogen and imaged with AFM.

3.3. Instrumentation

3.3.1. Rotator and rotating rod

The capture substrates were rotated with an AFMSRX analytical rotator from Pine Instrument Company. The rotator has an accuracy of 1% between 0 and 10,000 rpm. The slew rate of the motor is ~300,000 rpm/s; therefore, the desired rotation rate is effectively attained instantaneously for the rotation rates (50–1200 rpm) and incubation times (10–30 min) used in these experiments.

The capture substrate, as noted above, is attached to an E2M single-piece RDE (Pine Instrument Company) by double sided tape (3 M). This electrode readily mates with the AFMSRX rotator, having one end of the rod with a diameter of 6 mm that is clamped into the rotator and the other end of the rod (12 mm diameter) that not only fits into a sample well (17 mm diameter), but also closely matches the 1 cm × 1 cm capture substrate.

3.3.2. Atomic force microscopy

A MultiMode NanoScope IIIa SFM (Digital Instruments), equipped with a 150 μm scanner, was used to image viruses

bound to the capture substrates. The AFM was operated in TappingMode under ambient conditions. An Ultrasharp cantilever/tip (MikroMasch) with a length of 120–130 μm, a width of 32–38 μm, a thickness of 3.5–4.5 μm, a resonant frequency of 265–400 kHz and a spring constant of 20–75 N/m was used to image the substrates. The setpoint oscillation was set to 80% of the free oscillation amplitude and 25 μm^2 images were recorded at a scan rate of 1.5 Hz (512 lines scans per image and 512 data points per line). A 5 μm × 5 μm scan size was selected to image the substrates because it balances the merits of imaging as large of an area as possible, while still providing sufficient resolution to confidently use particle size in order to identify individual PPV particles when collecting 512 data points per line scan. The viruses in each topographic image were enumerated manually with a height scale of 20 nm using a pen style colony counter (Sigma).

3.4. Data analysis

Experimental counts of bound PPV/25 μm^2 were plotted versus the substrate rotation rate. The error in the measurements were assumed to follow a Poisson distribution predicted by counting statistics (Bevington, 1969), and is represented by the plotted error bars. Equations describing these curves were determined using the curve-fitting software provided with SigmaPlot 8.0, which relies on the Marquardt–Levenberg algorithm (Sigmaplot, 2002). The fits were performed with the default parameters of 100 iterations (maximum), a step size of 100 and a tolerance of 0.0001. The curves were fit with weight $1/y^2$ to account for differences in the uncertainty of each data point (Bevington, 1969). The coefficient of determination (r^2 value) was used to measure the fit of the calculated equation to the experimental data.

4. Results and discussion

The principal goal of this work was to develop a methodology to reduce the incubation time required for immunoassays by substrate rotation while maintaining satisfactory performance (e.g., detection limit). To achieve this goal, a key step is to gain an understanding of how best to implement rotation to control flux. The following sections therefore describe a detailed investigation of the relationship between capture substrate rotation rate and incubation time on PPV binding. First, experimental results are compared to theoretical predictions in order to substantiate the claim of controlled flux. Through curve fitting, it is possible to predict the PPV binding results for a given set of experimental conditions as well as extract the absolute solution concentration of virus in units of PPV/mL. Finally, the advantages of rotating a capture substrate are demonstrated by constructing a dose–response curve with and without substrate rotation.

4.1. Control of antigen extraction via substrate rotation and incubation time

Capture substrates were exposed to sample solutions of PPV (3.2×10^6 $TCID_{50}$/mL) with varying rotation rates and incubation times. A partial set of the resulting AFM images is presented in Fig. 3. As evident, PPV appears as a spherical object with a height of ~18 nm (topography cross-sections not shown). The height (*z*-direction) of the imaged PPV is consistent for all the particles but is slightly smaller than expected. This difference is a result from the dehydration of the ~25 nm viral particles on the substrate after drying. Note as well that the lateral size of the PPV varies in the *x*–*y* plane from image to image. This lateral variation is an artifact of tip convolution effects (Montelius and Tegenfeldt, 1993) and the use of different tips to image differ-

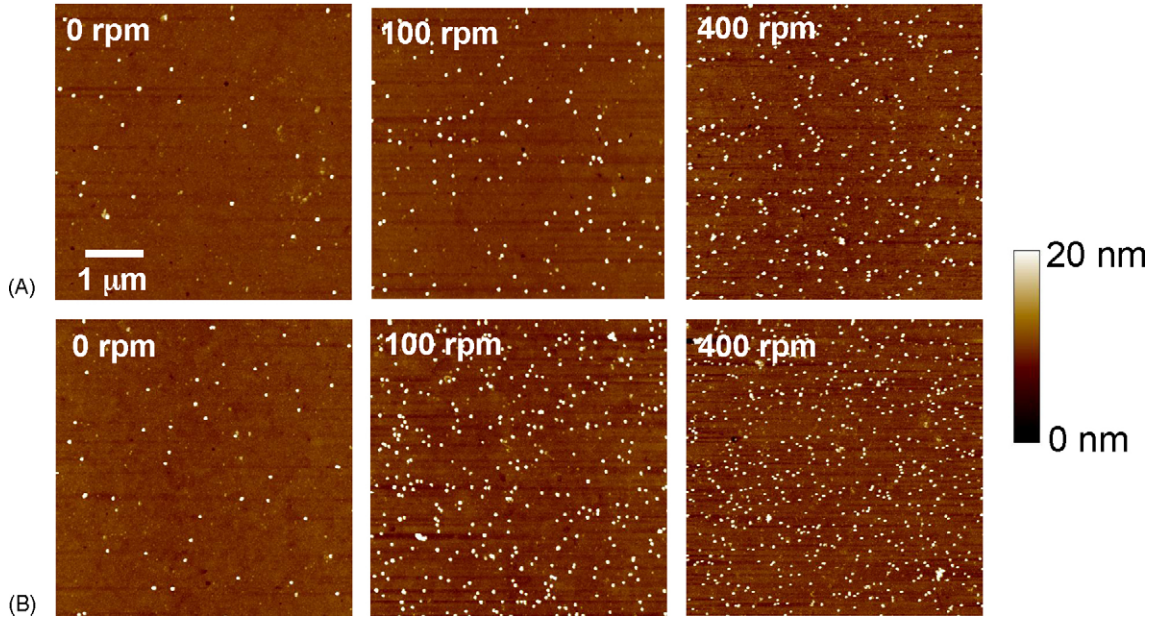

Fig. 3. AFM micrographs (5 μm × 5 μm) of PPV bound to capture substrates with an incubation time of: (A) 10 min and (B) 30 min. The capture substrate was either held stationary or rotated at 100 or 400 rpm.

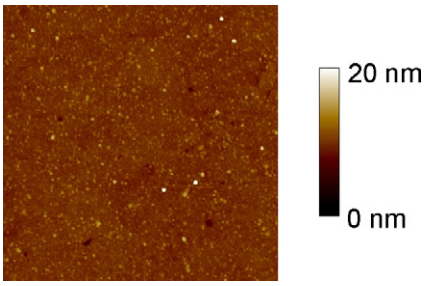

Fig. 4. AFM micrograph (5 μm × 5 μm) of an anti-FCV antibody modified capture substrate exposed to PPV demonstrating little nonspecific binding and confirming the specificity of the capture substrate.

ent samples. Importantly, the consistency in height allows for identification and enumeration of captured PPV.

The AFM images in Fig. 3 illustrate the effect of substrate rotation rate and sample incubation time on the number of viruses captured. The three images in Fig. 3A present the findings for a 10 min incubation in PPV for a stationary capture substrate and for substrates rotated at 100 and 400 rpm. Rotation significantly increases the number of viruses bound to the substrate. Moreover, a larger rotation rate results in a rise in the number of bound viruses. A similar trend is evident in the images in Fig. 3B for the 30 min incubations. Not surprisingly, when comparing images at the two different incubation times but same rotation rate, the longer incubation time leads to increased binding.

Control experiments were performed to verify the binding specificity between the capture substrate and PPV. To this end, capture substrates were coated with anti-FCV monoclonal antibodies (Driskell et al., 2005). This substrate was then rotated at 800 rpm for 10 min in a 3.2×10^6 $TCID_{50}$/mL sample solution of PPV. A representative AFM image is shown in Fig. 4, and as is evident, very few (<10) PPV are nonspecifically bound to the substrate. We therefore conclude that the PPV binding to anti-PPV antibody modified substrates, as in Fig. 3, is a result of specific interactions.

Fig. 5 plots the observed surface concentration of bound viruses (normalized to an area of 25 μm^2) versus rotation rate for both 10 and 30 min incubation times. Rotation rates up to 1200 rpm were tested. These plots, as expected, demonstrate that both incubation time and rotation rate can be used to control the number of viruses binding to the capture substrate. Interestingly, the plots appear to approach different limiting values of Γ_a. At some large rotation rate, both curves would reach the same value for Γ_a. However, the 30 min incubation plot would reach saturation at a slower rotation rate. A more detailed discussion of the shape of these profiles is given in the next section.

4.2. Validation of boundary conditions

A fit of the data plotted in Fig. 5 to Eq. (6), after validation of the boundary conditions imposed for its derivation, can be used to make predictions regarding the impact of changes in incubation time and rotation rate. The first boundary condition, the surface is not saturated with captured antigens, is validated

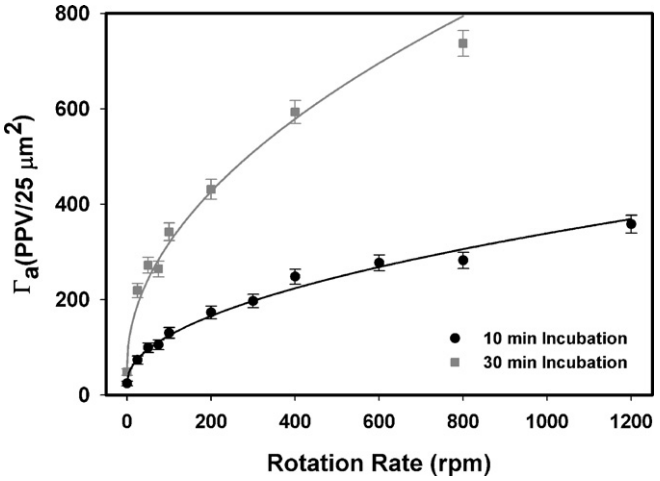

Fig. 5. The number of PPV bound to the capture substrates at varying rotation rates is plotted. Each plot is constructed from the average of two to three substrates at each rotation rate. Five AFM images from each capture substrate were then collected. The error bars represent the error introduced using Poisson statistics and the solid lines are weighted fits of the experimental data to Eq. (7) (see Section 3.4 for details on data analysis).

by the AFM findings (Fig. 3). Theoretically, a jamming limit treatment (Evans, 1993) indicates that $\sim 3 \times 10^4$ PPV can fit in a 25 μm^2 area. However, as exemplified by Fig. 5, no more than ~800 PPV were found in any 5 μm × 5 μm AFM image. The number of captured viruses is therefore only ~3% of that for a saturated substrate.

The second boundary condition requires that the extractive loss of PPV during incubation does not alter the bulk virus concentration. To test this assumption, a 3.2×10^6 $TCID_{50}$/mL solution of PPV (1.0 mL) was exposed to a rotating capture substrate (1200 rpm) for 10 min. This substrate was then replaced by a second rotating capture substrate (1200 rpm) and exposed to the same PPV sample for 10 min. Both substrates were then imaged with AFM to determine if the number of captured PPV on the second substrate differed from that of the first. A difference would point to a change in the bulk concentration of PPV as a consequence of extraction by the first substrate, and potentially invalidate the second assumption. A representative AFM image of each substrate is given in Fig. 6. The first substrate captured 346 ± 8 PPV/25 μm^2 and the second substrate bound 341 ± 16 PPV/25 μm^2. This result therefore supports the

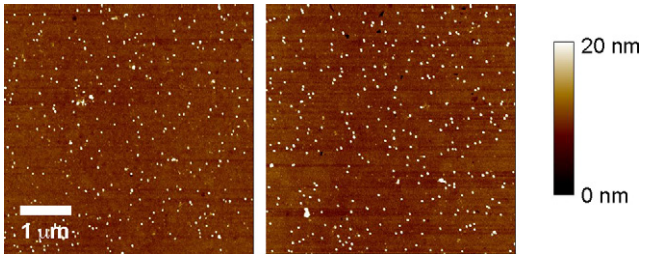

Fig. 6. AFM micrographs of successive exposure of two capture substrates (1200 rpm, 10 min incubation) to the same 3.2×10^6 $TCID_{50}$/mL PPV sample solution. The first substrate (left) was exposed to the original sample and captured 346 ± 8 PPV/25 μm^2. The second substrate (right) was exposed to the same PPV sample solution and bound 341 ± 16 PPV/25 μm^2.

assumption that the bulk PPV concentration is not reduced during the time of incubation.[1]

The third boundary condition, which pertains to the diffusion limited reaction rate for antigen–antibody binding, has been shown in multiple studies (Frackelton and Weltman, 1980; Myszka et al., 1997; Nygren et al., 1987; Stenberg and Nygren, 1985; Stenberg et al., 1986) and is most likely applicable in our system. As a result of validating the first two assumptions, demonstrating a close fit of the two profiles in Fig. 5 to Eq. (6) would strongly argue that the third assumption also holds. The two sets of experimental data plotted in Fig. 5 were fit to Eq. (7) by using the Marquardt–Levenberg algorithm (Sigmaplot, 2002), noting that the *a*-parameter represents the first term on the right side of Eq. (6) and the *b*-parameter stands for all remaining variables in the second term of the same equation.

$$\Gamma_a = a + b\omega^{1/2} \tag{7}$$

The best fit curves for 10 and 30 min incubation with the sample solutions are given by Eqs. (8) and (9), respectively,

$$\Gamma_a = 25 + 9.9\omega^{1/2} \tag{8}$$

$$\Gamma_a = 49 + 26\omega^{1/2} \tag{9}$$

where Γ_a is in units of PPV/25 μm^2 and ω is in units of rpm. Importantly, the calculated curves reasonably follow the experimental data ($r^2 = 0.9952$ for 10 min and $r^2 = 0.9873$ for 30 min), confirming the dependence of the bound PPV on the square root of rotation rate. Additionally, the best fit determination of parameter *b* for the 30 min incubation data is approximately three-fold greater than that for the 10 min incubation; this difference is consistent with the value of *b* being directly proportional to time. Moreover, the *a* term, determined from the best fits, is approximately proportional to $t^{1/2}$, as predicted by Eq. (6), but contains greater error since it is based only on two data points. This portion of the experiment is also complicated by the fact that immersion of the substrate disrupts the existence of a quiet solution. Taken together, the fit of the experimental data to Eq. (6) strongly supports the validity of the third boundary condition, providing yet another example of a heterogeneous immunoassay that is controlled by mass transfer rather than the rate of antibody–antigen recognition.

4.3. Relating $TCID_{50}$ and virus concentration

The strong correlation between the experimental data and best fit curves provides an alternative means for a determination of the relationship between the infective titration parameter ($TCID_{50}$/mL) and absolute PPV concentration (PPV/mL) by evaluating the second term in Eq. (6). All of the parameters in the second term, with the exception of C_b (PPV/mL), are known and the *b* value (Eq. (7)) is measured for both 10 and 30 min incubations. For the system presented, D_a is 1.75×10^{-7} cm^2/s (estimated using a hydrated radius of 12.5 nm via the Stokes–Einstein equation (Berry et al., 1980)), *V* is 1.004×10^{-2} cm^2/s at 25 °C and *t* is 10 or 30 min. Evaluation of Eq. (6), in light of the known parameters and the experimentally determined value of *b*, yields a bulk concentration of PPV of 4.3×10^9 and 4.9×10^9 PPV/mL for the 30 and 10 min incubation time plots, respectively.

As a means to validate the PPV concentration determined from the rotation study, experiments using exhaustive binding of PPV from a known sample volume to capture substrates were performed. These studies exposed a small volume sample of PPV (20 μL) to a capture substrate. After ~12 h of stagnant incubation, the sample solution was carefully removed from the substrate and dispensed onto a second substrate for another 12 h incubation. This process was repeated five times using five fresh capture substrates. All substrates were then imaged and the number of viruses bound in a 25 μm^2 area for five different locations on each sample was enumerated. The average number of PPV bound in the imaged area was then extrapolated to delineate the number bound in the entire 4.0 mm diameter address on the capture substrate. The results from each substrate were added to determine the total number of PPV present in the 20 μL of sample solution.

This experiment was performed twice. The first attempt, as shown by the set of AFM images in Fig. 7, yielded 187 ± 15 PPV/25 μm^2 on the first substrate, 3 ± 1 PPV/25 μm^2 on the second substrate, and no detectable PPV on all subsequent substrates. The second study captured 177 ± 15 PPV/25 μm^2 on the first substrate, 6 ± 2 PPV/25 μm^2 on the second substrate, and no detectable PPV on all subsequent substrates. The two exhaustive binding studies yielded PPV concentrations of $4.4 \pm 0.4 \times 10^9$ and $4.7 \pm 0.4 \times 10^9$ PPV/mL. These results are

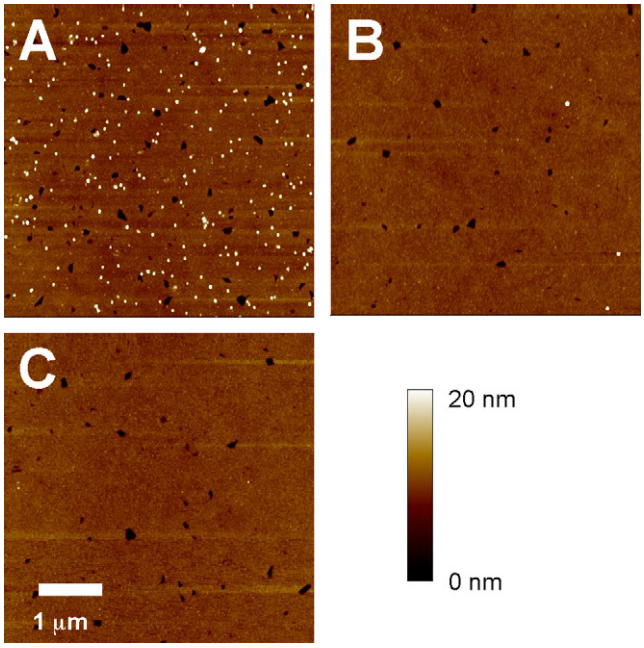

Fig. 7. Exhaustive binding of 20 μL of PPV (3.2×10^6 $TCID_{50}$/mL). The same sample was exposed to substrate (A) for ~12 h followed by subsequent exposure to substrates (B and C) for ~12 h each under stagnant conditions.

[1] Assays shown below captured as many as 800 PPV/25 μm^2. While those experiments extracted significantly more PPV than the ~340 PPV/25 μm^2 in these experiments, only ~8% of the PPV in the sample was extracted and therefore did not significantly alter the bulk concentration.

remarkably similar to the values of C_b calculated from the rotating substrate study, substantiating that the substrate rotation technique can be used as an absolute method for virus concentration determination.

The results from the substrate rotation study and exhaustive binding study indicate that the PPV concentration is between 4.3×10^9 and 4.9×10^9 PPV/mL. Since the specified concentration of PPV equaled 3.2×10^6 $TCID_{50}$/mL, 1 $TCID_{50}$/mL corresponds to 1300–1500 viruses/mL for PPV. $TCID_{50}$ is a measure of virus concentration based on the cytopathogenicity of a virus. However, different viruses have different inherent abilities infect and kill cells, and therefore the number of viruses that will cause cell death is specific for each virus (Wagner and Hewlett, 1999). Thus, the numerical quantities of two different viruses cannot be directly correlated by using values of $TCID_{50}$/mL and a comparison of analytical figures of merit between methodologies is difficult unless the same virus is used. We believe that the above approach, which establishes the first conversion (to our knowledge) between the quantal numeric of infective dose units and viral concentration in units of viruses/mL for PPV, will serve as a much needed means to broadly perform such determinations.

4.4. Dose–response curves and reductions in incubation time

Dose–response curves were constructed by exposing capture substrates to varying concentrations of PPV diluted in 10 mM PBS. Two sets of PPV binding experiments were carried out: one without substrate rotation and the other while the substrate was rotated at 800 rpm. All incubation times were held constant at 10 min, with AFM used for viral counting. Fig. 8 plots the results of this study.

As is evident, the immunoassay performed with substrate rotation is much more sensitive than that relying solely on analyte diffusion. Only a few virus-sized objects are found in the 25 μm^2 images of blanks, and are attributed to debris with a size comparable to PPV and/or to a small amount of contamination from transfer pipettes. Based on these results, the limit of detection, which is defined as the concentration yielding a signal equal to the blank signal plus three times its standard deviation, is 3.2×10^5 $TCID_{50}$/mL without rotation and 3.4×10^4 $TCID_{50}$/mL with rotation at 800 rpm. If we use the average of the two conversion factors determined earlier, these results correspond to a limit of detection of 4.9×10^7 PPV/mL (~80 fM) with rotation and 4.6×10^8 PPV/mL (~800 fM) without rotation.

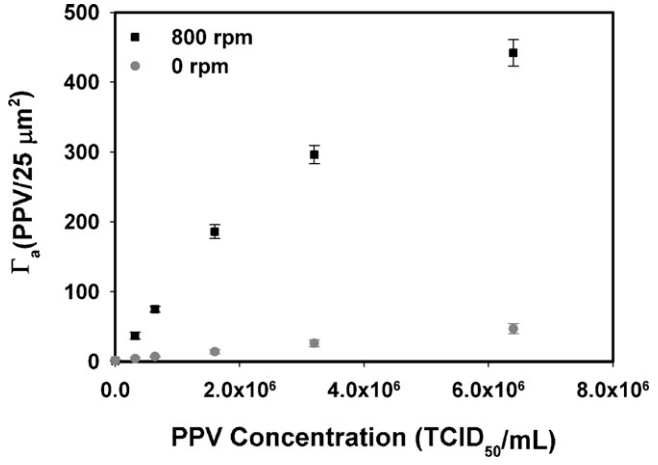

Fig. 8. Dose–response curves for immunoassays performed under stagnant conditions and with capture substrate rotation at 800 rpm. The sample volume was 1.0 mL and the incubation time was 10 min. Each data point is the average signal measured from five different locations on the same sample substrate and the standard deviations are represented by the error bars.

There is one other interesting, but not yet understood, observation from the plots in Fig. 8. The response is linear for the immunoassay performed without rotation throughout the concentration range tested, while that with rotation is linear in the lower concentration range but begins to negatively deviate at high concentrations. Linearity is expected in both cases in accordance with Eq. (6), and we are currently working to identify experiments that may provide insight into the observed deviation.

Finally, the overall approach to this assay has a strongly predictive value in that the experimental conditions can be tailored via Eq. (6) to obtain the desired result. If, for example, all the known parameters for the PPV assay are incorporated into Eq. (6), we can write,

$$\Gamma_a = C_b(1.6 \times 10^{-9} t^{1/2} + 2.0 \times 10^{-10} t\omega^{1/2}) \quad (10)$$

where Γ_a is in PPV/25 μm^2, t in minutes, C_b in PPV/mL and ω is in rpm. Eq. (10) provides the flexibility to calculate: (1) the necessary rotation rate to detect a given C_b in a predetermined incubation time, (2) the limit of detection, C_b, at a fixed rotation rate and incubation time or (3) the time required to detect a desired C_b with a set rotation rate. We believe that the predictive nature of this system will facilitate its extension to many other types of immunoassays.

5. Conclusions

Substrate rotation can be used to increase antigen flux to the capture surface in a heterogeneous immunoassay. While the actual hands-on time to perform the rotated experiments is equivalent to a traditional stagnant assay, substrate rotation eliminates the long incubation periods, significantly reducing the total assay time. Thus, analysis throughput is readily increased. Substrate rotation also led to an improvement in the analytical performance of the presented AFM-based immunoassay, resulting in a 10-fold reduction in the limit of detection for the model study reported herein. With rotation, the flux of the antigen can also be controlled and employed to predict and design optimized immunoassays. Due to the predictive nature of the system, it was possible to determine the concentration of PPV in an unknown sample solution without the use of standards and to develop an approach to convert quantal metrics to actual antigen concentrations. Moreover, the ability to quantitate the number of viruses per unit volume is necessary to assess and compare analytical performance and in order to accurately determine the total

nucleic acid or capsid protein content in a particle for determinations of virus structure. Furthermore, these significant benefits resulting from substrate rotation were achieved utilizing simple, inexpensive (∼US$ 10,000) instrumentation that is commonly found in many chemistry laboratories. Experiments to apply this concept to more challenging sample types and matrices are planned.

Acknowledgments

The authors would like to thank A.J. Bergren for helpful discussions regarding the theory. This work was supported through a grant from USDA-NADC and by the Institute for Combinatorial Discovery of Iowa State University. J.D.D. would like to gratefully acknowledge the support of the Mary K. Fassel and Velmer A. Fassel Fellowship. K.M.K. would like to recognize the gracious support of a Dow Chemical Fellowship. The Ames Laboratory is operated for the U.S. Department of Energy by Iowa State University under contract W-7405-eng-82.

References

Bard, A.J., Faulkner, L.R., 2001. Electrochemical Methods Fundamentals and Applications. John Wiley & Sons, New York.

Berry, R.S., Rice, S.A., Ross, J., 1980. Physical Chemistry. John Wiley & Sons, New York.

Bevington, P.R., 1969. Data Reduction and Error Analysis for The Physical Sciences. McGraw-Hill, New York.

Cao, Y.C., Jin, R., Mirkin, C.A., 2002. Nanoparticles with raman spectroscopic fingerprints for DNA and RNA detection. Science 297, 1536–1540.

Chen, C.S., Mrksich, M., Huang, S., Whitesides, G.M., Ingber, D.E., 1998. Micropatterned surfaces for control of cell shape, position, and function. Biotechnol. Prog. 14, 356–363.

Chomel, B.B., 2003. Control and prevention of emerging zoonoses. J. Vet. Med. Educ. 30, 145–147.

Cousino, M.A., Jarbawi, T.B., Halsall, H.B., Heineman, W.R., 1997. Pushing down the limits of detection: how low can anlaytical chemistry go? Anal. Chem. 69, 544A–549A.

Diamandis, E.P., Christopoulos, T.K., 1996. Past, present and future of immunoassays. In: Diamandis, E.P., Christopoulos, T.K. (Eds.), Immunoassay. Academic Press, San Diego, CA, pp. 1–3.

Donaldson, K.A., Kramer, M.F., Lim, D.V., 2004. A rapid detection method for vaccinia virus, the surrogate for smallpox virus. Biosens. Bioelectron. 20, 322–327.

Driskell, J.D., Kwarta, K.M., Lipert, R.J., Porter, M.D., Neill, J.D., Ridpath, J.F., 2005. Low level detection of viral pathogens by a surface-enhanced raman scattering based immunoassay. Anal. Chem. 77, 6147–6154.

Duhachek, S.D., Kenseth, J.R., Casale, G.P., Small, G.J., Porter, M.D., Jankowiak, R., 2000. Monoclonal antibody-gold biosensor chips for detection of depurinating carcinogen–DNA adducts by fluorescence line-narrowing spectroscopy. Anal. Chem. 72, 3709–3716.

Evans, J.W., 1993. Random and cooperative sequential adsorption. Rev. Mod. Phys. 65, 1281–1329.

Ewalt, K.L., Haigis, R.W., Rooney, R., Ackley, D., Krihak, M., 2001. Detection of biological toxins on an active electronic microchip. Anal. Biochem. 289, 162–172.

Ferguson, J.A., Steemers, F.J., Walt, D.R., 2000. High-density fiber-optic DNA random microsphere array. Anal. Chem. 72, 5618–5624.

Frackelton, A.R., Weltman, J.K., 1980. Diffusion control of the binding of carcinoembryonic antigen (cea) with insoluble anti-cea antibody. J. Immunol. 124, 2048–2054.

Glaser, R.W., 1993. Antigen–antibody binding mass transport by convection and diffusion to a surface: a two-dimensional computer model of binding and dissociation kinetics. Anal. Biochem. 213, 152–161.

Grubisha, D.S., Lipert, R.J., Park, H.-Y., Driskell, J., Porter, M.D., 2003. Femtomolar detection of prostate-specific antigen: an immunoassay based on surface-enhanced raman scattering and immunogold labels. Anal. Chem. 75, 5936–5943.

Heller, M.J., Forster, A.H., Tu, E., 2000. Active microelectronic chip devices which utilize controlled electrophoretic fields for multiplex DNA hybridizaion and other genomic applications. Electrophoresis 21, 157–164.

Hofmann, O., Voirin, G., Niedermann, P., Manz, A., 2002. Three-dimensional microfluidic confinement for efficient sample delivery to biosensor surfaces. Application to immunoassays on planar optical waveguides. Anal. Chem. 74, 5243–5250.

Huet, D., Gyss, C., Bourdillon, C., 1990. A heterogeneous immunoassay performed on a rotating carbon disk electrode with electrocatalytic detection. J. Immunol. Meth. 135, 33–41.

Johnstone, R.W., Andrew, S.M., Hogarth, M.P., Pietersz, G.A., McKenzie, I.F.C., 1990. The effect of temperature on the binding kinetics and equilibrium constants of monoclonal antibodies to cell surface antigens. Mol. Immunol. 27, 327–333.

Jones, V.W., Kenseth, J.R., Porter, M.D., Mosher, C.L., Henderson, E., 1998. Microminiaturized immunoassays using atomic force microscopy and compositionally patterned antigen arrays. Anal. Chem. 70, 1233–1241.

Kjeldsberg, E., 1986. Demonstration of calicivirus in human faeces by immunosorbent and immunogold-labelling electron microscopy methods. J. Virol. Meth. 14, 321–333.

Kumar, A., Whitesides, G.M., 1993. Features of gold having micrometer to centimeter dimensions can be formed through a combination of stamping with an elastomeric stamp and an alkanethiol "ink" followed by chemical etching. Appl. Phys. Lett. 63, 2002–2004.

Kuznetsov, Y.G., Malkin, A.J., Lucas, R.W., Plomp, M., McPherson, A., 2001. Imaging of viruses by atomic force microscopy. J. Gen. Virol. 82, 2025–2034.

Levich, V.G., 1962. Convective Diffusion in Liquids. Prentice-Hall, Englewood Cliffs, NJ.

Libioulle, L., Bietsch, A., Schmid, H., Michel, B., Delamarche, E., 1999. Contact-inking stamps for microcontact printing of alkanethiols on gold. Langmuir 15, 300–304.

Llic, B., Yang, Y., Craighead, H.G., 2004. Virus detection using nanoelectromechanical devices. Appl. Phys. Lett. 85, 2604–2606.

Mengeling, W.L., Ridpath, J.F., Vorwald, A.C., 1988. Size and antigenic comparisons among the structural proteins of selected autonomous parvoviruses. J. Gen. Virol. 69, 825–837.

Messina, G.A., Torriero, A.A.J., DeVito, I.E., Olsina, R.A., Raba, J., 2005. Continuous-flow/stopped-flow system using an immunobiosensor for quantification of human serum igg antibodies to *Helicobcter pylori*. Anal. Biochem. 337, 195–202.

Montelius, L., Tegenfeldt, J.O., 1993. Direct observation of the tip shape in scanning probe microscopy. Appl. Phys. Lett. 62, 2628–2630.

Murphy, F.A., Gibbs, E.P.J., Horzinek, M.C., Studdert, M.J., 1999. Veterinary Virology. Academic Press, San Diego.

Myszka, D.G., Morton, T.A., Doyle, M.L., Chaiken, I.M., 1997. Kinetic analysis of a protein antigen–antibody interaction limited by mass transport on an optical biosensor. Biophys. Chem. 64, 127–137.

Nettikadan, S.R., Johnson, J.C., Mosher, C., Henderson, E., 2003. Virus particle detction by solid phase immunocapture and atomic force microscopy. Biochem. Biophys. Res. Commun. 311, 540–545.

Nygren, H., Werthen, M., Stenberg, M., 1987. Kinetics of antibody binding to solid-phase-immobilized antigen: effect of diffusion rate limitation and steric interaction. J. Immunol. Meth. 101, 63–71.

Opekar, F., Beran, P., 1976. Rotating disk electrodes. J. Electroanal. Chem. 69, 1–105.

Reed, L.J., Muench, H., 1938. A simple method of estimating fifty percent endpoints. Am. J. Hyg. 27, 493–497.

Richardson, J., Hawkins, P., Luxton, R., 2001. The use of coated paramagnetic particles as a physical label in a magneto-immunoassay. Biosens. Bioelectron. 16, 989–993.

Rieger, P.H., 1994. Electrochemistry. Chapman & Hall, New York.

Salinas, E., Torriero, A.A.J., Sanz, M.I., Battaglini, F., Raba, J., 2005. Contiuous-flow system for horseradish peroxidase enzyme assay comprising a packed-column, and amperometric detector and a rotating bioreactor. Talanta 66, 92–102.

Sheehan, P.E., Whitman, L.J., 2005. Detection limits for nanoscale biosensors. Nano Lett. 5, 803–807.

Sigmaplot 8.0. SPSS Inc., Chicago, IL.

Sokoll, L.J., Chan, K.W., 1999. Clinical analysers. Immunoassays. Anal. Chem. 71, 356R–362R.

Stamou, D., Gourdon, D., Liley, M., Burnham, N.A., Kuik, A., Vogel, H., Duschl, C., 1997. Uniformly flat gold surfaces: imaging the domain structure of organic monolayers using scanning force microscopy. Langmuir 13, 2425–2428.

Stenberg, M., Nygren, H., 1985. A diffusion limited reaction theory for a solid-phase immunoassay. J. Theor. Biol. 113, 589–597.

Stenberg, M., Stiblert, L., Nygren, H., 1986. External diffusionin solid-phase immunoassays. J. Theor. Biol. 120, 129–140.

Wagner, E.K., Hewlett, M.J., 1999. Basic Virology. Blackwell Sciences Inc., Malden, MA.

Wagner, P., Hegner, M., Kernen, P., Zaugg, F., Semenza, G., 1996. Covalent immobilization of native biomolecules onto au(1 1 1) via *n*-hydroxysuccinimide ester functionalized self-assembled monolayers for scanning probe microscopy. Biophys. J. 70, 2052–2066.

Wang, H., Branton, D., 2001. Nanopores with a spark for single-molecule detection. Nat. Biotechnol. 19, 622–623.

White, S.R., Chiu, N.H.L., Christopoulos, T.K., 2000. Expression immuoassay. Methods 22, 24–32.

Wijayawardhana, C.A., Purushothama, S., Cousino, M.A., Halsall, H.B., Heineman, W.R., 1999. Rotating disk electrode amperometric detection for a bead-based immunoassay. J. Electroanal. Chem. 468, 2–8.

Zheng, Y.Z., Hyatt, A., Wang, L.-F., Eaton, B.T., Greenfield, P.F., Reid, S., 1999. Quantification of recombinant core-like particles of bluetongue virus using immunosorbent electron microscopy. J. Virol. Meth. 80, 1–9.